Dynamical self-consistent description of exotic structures in nuclear matter at subnuclear densities

Virginia de la Mota, François Sébille and Sébastien Figerou
SUBATECH, Université de Nantes-IN2P3(CNRS)-EMN, Nantes, France

Abstract
We investigate the occurrence of exotic structures in nuclear matter at subnuclear densities within the framework of the **dywan** model. This approach, developed ab initio for the description of nuclear collisions, is a microscopic dynamical approach in which the numerical treatment makes use of wavelet representation techniques. Before tackling the effects of multi-particle correlations on the overall dynamics, we focused the present work on the study of cold matter within a pure mean field description. Starting from inhomogeneous initial conditions provided by an arrangement of nuclei located on an initial crystalline lattice, the exotic structures result from the dynamical self-consistent evolution. The nuclear system can freely self-organize, it can modify or even break the lattice structure and the initial symmetries of matter distribution. This approach goes beyond the Wigner-Seitz approximation and no assumption of final shapes of matter is made. In this framework, different effects, as the sensitivity of the structural phases to the Equation of State and to the proton fraction are analysed.

1 Introduction

Neutron stars have fascinated scientists since their discovery in the last century, and a considerable effort has been done in order to understand its peculiar observed behaviour. In addition, at present there is an increasing amount of observational data from terrestrial and from satellital telescopes as well.

Neutron stars are the remnant which is left behind the explosion of massive stars. Since they are very compact objects, they constitute a true laboratory for the study of dense matter.
It is usual to divide neutrons stars in different regions according with their density. The outermost layer, of about 0.5 km thick and mean density $< \rho > \lesssim 10^{11}$g cm^{-3}, is supposed to be composed of essentially a crystalline lattice of neutron-rich nuclei immersed in a degenerate gas of electrons. The inner part of the crust, around 1km thick, is still composed by nuclei in the electron gas background and, in addition, by a gas composed by dripped neutrons. There the density ranges between 4×10^{11}g cm^{-3} and 1×10^{14}g cm^{-3}. After this region there is the core, where matter is supposed to be composed of a uniform liquid of neutrons, protons and electrons and, possibly, other elementary particles can appear as density increases, when going to the center of the star. The thickness of this region is around 10 km and the density is supposed to increase up to $\sim 10^{15}$g cm^{-3} and higher.

We will focus ourselves on the crust, which corresponds to roughly the two first mentioned regions. In this region the existence of nuclei with exotic shapes has been predicted independently by Refs. [1] and [2], both works based on a liquid-drop description. These non spherical shapes, which have been called “pasta phases”, are supposed to occur at sub-nuclear densities, as the result of the interplay between Coulomb and nuclear forces. It has been argued that the occurrence of these structures can influence the observation of different internal processes, as the interaction of neutrinos with matter [3], [4], and that they could be sensitive to the equation of stare (EOS) of nuclear matter.

That pioneer prediction has been confirmed by recent works, in particular by that of Ref. [3] where the importance of nuclear dynamics has been underlined. Most theoretical works agree in the following scheme giving the evolution of the structures with increasing density:

spherical $\rightarrowtail$ cylinders $\rightarrowtail$ slabs $\rightarrowtail$ complex structures $\rightarrowtail$ uniform.

The aim of this work is to study the properties of matter as it could exist in the crust, in particular we would like to understand the occurrence and evolution of non-spherical phases. In the present range of temperatures (T$\sim$ 1 MeV) and densities ($\rho \lesssim \rho_\infty$), matter is correctly described in terms of interacting nucleons in a uniform distribution of electrons [5]. To this end we have developped a new model which is based on the **dywan** model of nuclear collisions [6]. Since the different structural phases involve low energy configurations, in this first calculations, we will investigate the role of a pure mean field description at zero temperature. In particular, we are interested in probing the sensitivity of the structures to the EOS of nuclear matter.

This work is organized as follows. In Section 2 the model is briefly presented. In Section 3 we present the results concerning some static properties of nuclear matter and the dynamical investigation of structures formation. Conclusions and outlooks are given in Section 4.

2 The model

At neutron star densities and temperatures nuclear matter can be modelled by a neutral mixture of nuclei, electrons and, eventually, free neutrons. Nuclei are expected to form a crystalline lattice and electrons are considered as a degenerate relativistic gas, modelled by a uniform charge density which ensures the neutrality of the system. The structure of the model consists into two main parts, the first one concerns the preparation of the initial state of the system, the second one its subsequent evolution.

2.1 Initial configuration

In a first step, a static Hartree-Fock (HF) self-consistent procedure is implemented in order to get nuclear composites either at their ground states or in excited states induced according to mechanical or thermal constraints. Each of these nuclei, prepared in a single Wigner-Seitz (WS) cell, are used to construct the super-cell (see Fig. 1) and with it the complete three-dimensional lattice, to which periodic boundary conditions are applied. For this calculation a simple cubic super-cell has been considered, but the characteristics of it can be arbitrarily chosen.

For this calculation we have chosen a density-dependent zero-range effective interaction, with the following self-consistent field:

$$\begin{aligned} V_q^{HF}(\rho,\xi) \;&=\; \frac{t_0'}{\rho_\infty}\,\rho \;+\; \frac{t_3'}{\rho_\infty^{\nu+1}}\,\rho^{\nu+1} \;+\; \frac{c}{{\rho_\infty}^2}\xi^2 \;+\; \frac{4qc}{{\rho_\infty}^2}\rho\xi \;+ \\ & \frac{\Omega}{3{\rho_\infty}^2}\xi^2 + \frac{4q\Omega}{3{\rho_\infty}^2}(\rho-\rho_\infty)\xi + V_q^C , \end{aligned} \tag{1}$$

where ρ_n and ρ_p stand for neutron and proton densities, $\rho = \rho_n \,+\, \rho_p$, $\xi = \rho_n \,-\, \rho_p$, q=1/2 for neutrons and -1/2 for protons, ρ_∞=0.145 fm^{-3} is the saturation density of infinite nuclear matter and V_q^C is the coulomb potential.

The parameters of the force are related with those corresponding to the usual Skyrme force, t_0, t_3, x_0 and x_3, by the following relationships:

$$t_0' = \frac{3\rho_\infty}{4}t_0 \qquad t_3' = \frac{3(\nu+2)\rho_\infty^{\nu+1}}{48}t_3 \;,$$

with $x_0 = x_3 = -1/2$. The values of these parameters are ν=1/6, c=20MeV, and:

$$t_0'/\rho_\infty = -356\mathrm{MeV\ fm}^3 \qquad t_3'/\rho_\infty^{\nu+1} = 303\mathrm{MeV\ fm}^{3(\nu+1)} \;.$$

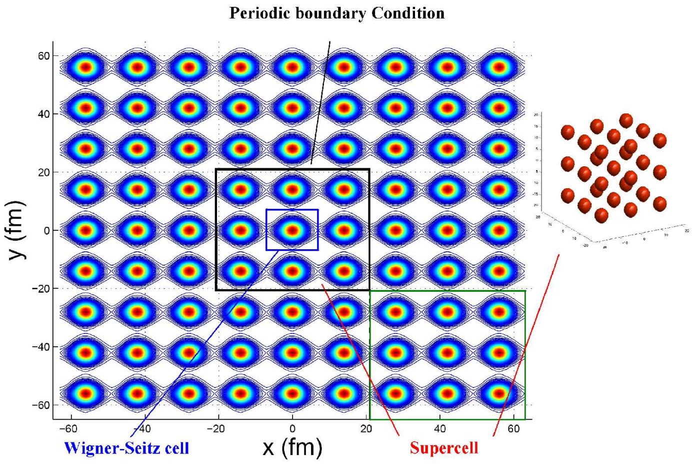

Fig. 1: Initial lattice density profiles. Wigner-Seitz cell and super-cell are displayed. Infinite matter is simulated through periodic boundary conditions.

The current values of the parameters reproduce the principal static characteristics of nuclei, as binding energies, radii and equilibrium densities. The incompressibility modulus in symmetric matter is K_∞= 200 MeV, corresponding to a soft EOS. The asymmetry parameter Ω will be varied in order to analyze the influence of the isospin dependence of the force on the morphological characteristics of matter.

2.2 Dynamical evolution

Once the initial conditions are given, nuclei are led to evolve allowing the matter to self-organize in a dynamical way. Using many-body techniques, as the projection methods, it is possible to derive a hierarchy of equations of motion for the reduced density matrices, which can be truncated under some assumptions, concerning the available information about the system. In this work we will remain at the lowest level of this hierarchy, which corresponds to a pure mean-field description. In this approach, single particle wavefunctions are spanned in a moving basis of wavelets $\{\alpha_i\}$:

$$|\varphi_\lambda > (t) = \sum_i c_i^\lambda |\alpha_i^\lambda > (t) \; . \tag{2}$$

Wavelets [8] are functions of a set of correlated coordinates $\{\vec{\xi}, \vec{\chi}, \vec{\pi}, \vec{\phi}\}$, which are the first and second moments in phase space:

$$< x >= \xi_x \quad < (x-\xi_x)^2 >= \chi_x \quad < p_x >= \pi_x \quad < (p_x-\pi_x)^2 >= \phi_x \; ,$$

with similar expressions for y and z components. The equations of motion of the moving basis can be obtained from a viariational principle [9]:

$$\dot{\xi} = \frac{\pi}{m} + \frac{\partial}{\partial \pi}\mathcal{V} \tag{3}$$

$$\dot{\pi} = -\frac{\partial}{\partial \xi}\mathcal{V} \tag{4}$$

$$\dot{\chi} = \frac{4\gamma\chi}{m} - \frac{\partial \mathcal{V}}{\partial \gamma} \tag{5}$$

$$\dot{\gamma} = \frac{\hbar^2}{8m\chi^2} - \frac{2\gamma^2}{m} - \frac{\partial}{\partial \chi}\mathcal{V} \; . \tag{6}$$

$\mathcal{V}$ being the wavelet transform of the effective nuclear potential $\mathcal{V} =< \alpha|V^{HF}|\alpha >$. It is important to underline that the self-consistent mean-field is a function of the density extended to the overall supercell and not only to a single WS cell.
Equations 4-6 are Hamilton like equations for the centroïds and widths of the moving basis and solve the TDHF equations for the single particle wave-functions [9].

3 Results

3.1 Static characteristics of nuclear matter

Among the principal physical quantities reflecting the characteristics of the force we can consider the energy per baryon ω and the chemical potential of pure neutron matter μ_n, which are defined as follows:

$$\omega = \frac{\varepsilon}{\rho} = \frac{\int V_q^{HF}\, d\rho}{\rho} + \omega_{kin} \qquad \mu_n = \frac{\partial \varepsilon}{\partial \rho_n}\,,$$

where the quantity ω_{kin} corresponds to the kinetic contribution to the density energy.
On the left part of Fig. 2 we represented the values of $\omega(\rho)$ in pure neutron matter for different values of

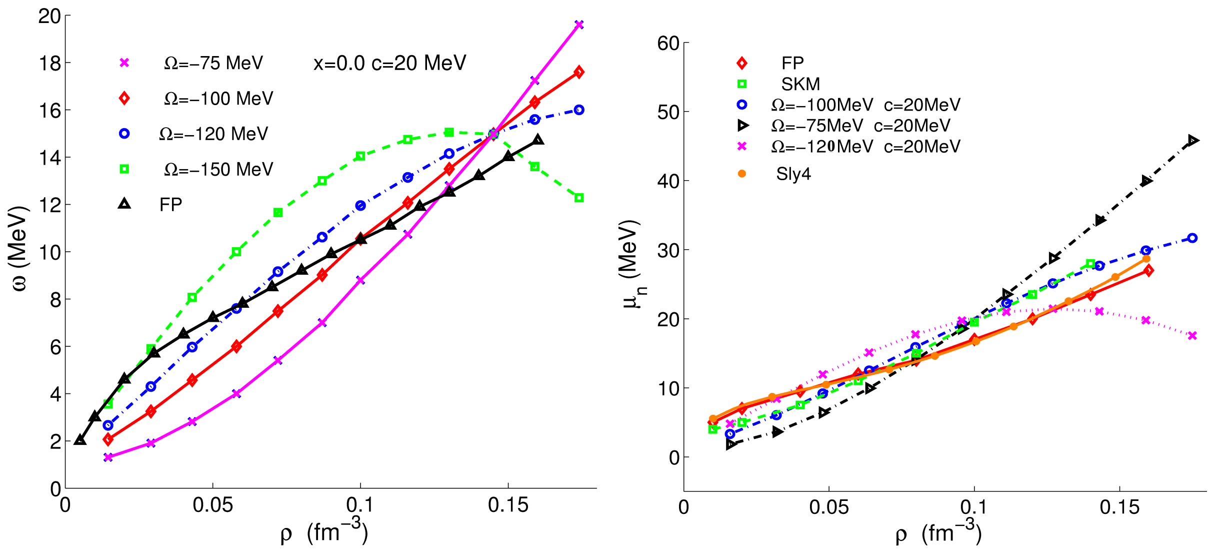

Fig. 2: Energy density per baryon (left) and neutron chemical potential (right) in cold neutron matter as a function of the density for different values of the asymmetry parameter Ω.

the asymmetry parameter Ω and with c=20 MeV. Together with these values are plotted the results of Ref. [10] in triangles. It can be shown that when the densities reach their respective saturation values in symmetric nuclear matter we obtain similar values of ω as those of the above reference.

On the right part of Fig. 2 is represented the neutron chemical potential as a function of the density in pure neutron matter. These calculations are also performed at zero temperature and for different values of Ω, for the same fixed c value. The results of References [10], [11] and [12] are in diamonds, squares and dots, respectively. The calculated values of μ_n with $\Omega = -100$MeV are in good agreement with SKM calculations, while those for the two other values of Ω show important differences with them mainly at high density. These differences will affect the dynamical evolution.

3.2 Dynamic behaviour

In Fig. 3 we show the time evolution of neutron density on a simple cubic supercell. The system is composed of 27 nuclei of oxigen isotopes, with proton fraction x=0.1. Individual nuclei have been initially prepared with a slight deformation and then released. Besides spherical shapes, the occurrence

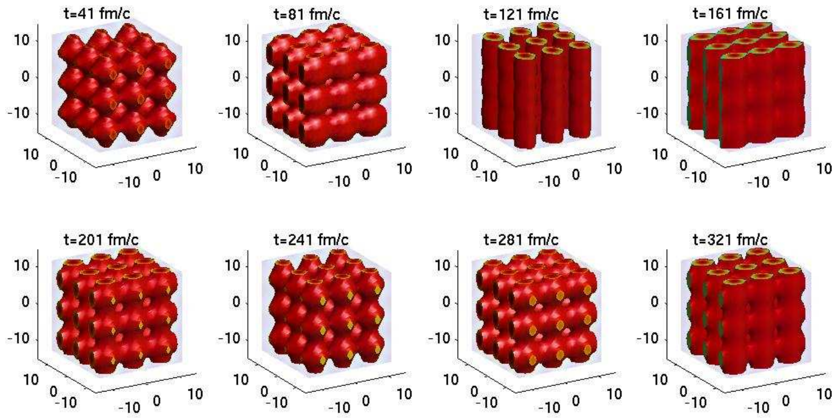

Fig. 3: Time evolution of the supercell neutron density correspondig to a system of 27 oxigen isotopes with proton fraction x=0.1.

of cylindrical or planar structures are observed as the transitions betwen these different shapes as well. In order to characterize these structures we have applied a methodology based on the integral-geometry morphological image analysis (MIA) [13], which assigns numbers to the different shapes [9].
Each plot stands for isodensity surfaces representing surfaces of equal density, which are higer than a given threshold density ρ_t. In Fig. 3 the corresponding threshold is ρ_t=0.065 fm^{-3}, while the overall mean density is $<\rho>$=0.0725 fm^{-3}.
The resulting density plots represent embedded structures, which are evidenced when varying the threshold density. This aspect is illustrated in Fig. 4 where we have represented the same system as in Fig. 3, at t=201fm/c, but with two different choices of ρ_t . In Fig. 3 ρ_t=0.065 and the structure can be char-

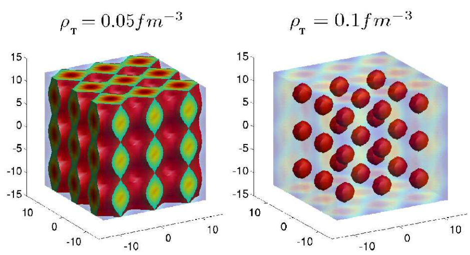

Fig. 4: Neutron density for the same system as in Fig. 3 at t=201 fm/c for two values of the threshold denstity ρ_t.

acterized as sponge-like, while in Fig. 4 the shapes are spherical, with ρ_t==0.09 fm^{-3} and cylindrical bubbles with ρ_t==0.05 fm^{-3}.

In order to get a better understanding about the interplay between these different aspects in Fig. 5 we have represented the different structures in a plot of the threshold density ρ_t versus the overall mean density $<\rho>$ for two proton fractions and for different values of the asymmetry parameter Ω.

For simplicity, we have considered a coarse-grained classification of phases: spherical (black), cylindrical (light grey), planar (dark grey), sponge-like structures (white) and bubbles (grey). In these

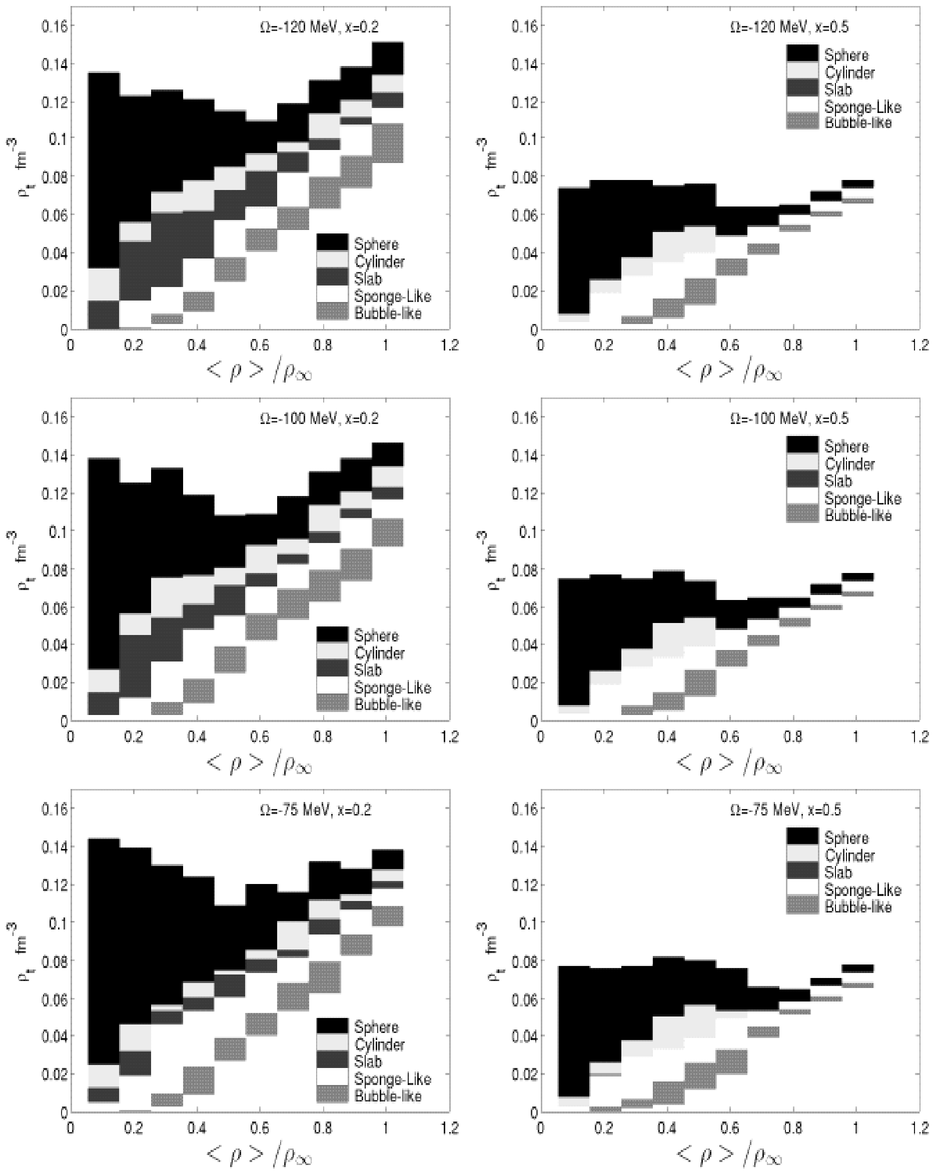

Fig. 5: Neutron threshold density versus the neutron mean density normalized to the saturation value for different values of Ω and for two proton fractions : x=0.2 (left) and x=0.5 (right). The different structures are in grey scale.

calculations we have implemented three different versions of the asymmetry parameter Ω in order to analyze the sensitivity of the results to the EOS, while keeping fixed the other parameters of the force.
As mentioned before, we observe in these pictures that for a fixed mean density different structures can coexist. Conversely, for a given value of threshold density ρ_t and for growing values of the average density the system takes successively different structures. For instance in the case Ω=-100MeV, x=0.2 (on the left) and a for a fixed value of ρ_t at around 0.06, the system passes through the above mentioned structures and in that order. This behaviour is in agreement with the typical picture of phases sorting suggested by the pioneer works of Ref. [1], [2] and confirmed by recent works. Among them we can mention the work of Ref. [3] where complex structures as sponge-like structures have been found, and they have been called "intermediate phases". The phase diagrams in this works are given in a one dimension representation. In our case, phase diagrams are two-dimentional and in Fig. 5 equivalent

structures to those of Ref. [3] can be observed along the density axis for a bin in the threshold density of around 0.06 fm^{-3} in the case where Ω=-100MeV and x=0.2.
In the symmetric case (on the right) the diagram is weakly dependent on the EOS and some structures are absent (slabs). In the asymetric case (on the left) more distinct structures can exist and more complex structures appear on a larger region of neutron threshold densities. In this case the influence of the EOS is more perceptible. Indeed, one observes that as the force softens (for increasing Ω values), the slab region increases and the one corresponding to sponge-like phases decreases.
This result can be related to the static characteristics of the force. Indeed, according to Fig. 2, the density variation of the neutron chemical potential in pure neutron matter is stronger for the stiffest effective interaction. Therefore, the emission of neutrons located near the surface will be favoured, or equivalently, the probability that neutron wave functions spread in all directions will increase. This is emphasised by a clear increase of sponge-like structures, in correlation with a greater spatial extension of the neutron liquid, linking the residual clusters. For this reason, the minimum threshold density for the onset of spherical structures is lowered.

4 Conclusion

The previous discussions indicate that the formation of non spherical phases and the transitions between them are processes of dynamical nature and that different morphological structures corresponding to different threshold densities can exist at a given time, for a given average density. The existence of these embedded structures makes their characterisation not trivial, for this reason it is worthwile to repesent them through phase diagrams in two dimensions. The observed structures are sensitive to both the proton fraction and to the EOS, mainly in the case of asymetric matter.
Nevertehless, several improvements have to be done, in order to go beyond a pure mean-field description. This requires a convenient treatment of particle correlations in the interest of introducing disspative effects and density fluctuations. On the other side it is necessary to implement more sophisticated effective forces and to diversify the crystalline lattice by introducing more complex cells. We are currently considering other initial conditions with more heavy nuclei subjected to different excitations. This work is in progress.

References

[1] D.G. Ravenhall, C.J. Pethick, and J.R. Wilson, Phys. Rev. Lett. **50** (1983) 2066.
[2] M. Hashimoto, H. Seki and M. Yamada, Prog. Theor. Phys. **71** (1984) 320.
[3] G. Watanabe et al. Phys. Rev. C **66** (2002) 012801(R).
[4] C.J. Horowitz, M.A. Pérez-Garcia and J. Pieckarewicz, Phys. Rev. C **69** (2004) 045804.
[5] J.W. Negele and D. Vautherin, Nucl. Phys. A **207** (1973) 298.
[6] B. Jouault, F. Sébille and V. de la Mota, Nucl. Phys. A **628** (1998) 119.
[7] M. Farine et al, Z. Phys. **A** 339 (1991) 363.
[8] M.Unser and A. Aldroubi, Polynomial splines and wavelets- A signal processing perspective in Wavelets: A tutorial in Theory, Ed. C.K. CHUI, Academic Press (1992) 91-122.
[9] F. Sébille, F. Figerou and V. de la Mota, Nucl. Phys. **A** 822 (2009) 51.
[10] B. Friedman, V.R. Pandharipande, Nucl. Phys. A **361** (1981) 501.
[11] H. Krivine, J. Treiner and O. Bohigas, Nucl. Phys. A **336** (1980) 155.
[12] F. Douchin, P. Haensel, Phys. Lett. B **435** (2000) 107.
[13] K. Michielsen and H. De Raedt, Phys. Rep. **347** (2001) 461.